Available online at www.sciencedirect.com
SCIENCE DIRECT
ELSEVIER
International Journal of Mass Spectrometry 249–250 (2006) 321–329
International Journal of Mass Spectrometry
www.elsevier.com/locate/ijms

Effects of projectile orientation and surface impact site on the efficiency of projectile excitation in surface-induced dissociation Protonated diglycine collisions with diamond {1 1 1}

Asif Rahaman, Jing Brian Zhou [1], William L. Hase *

Department of Chemistry and Biochemistry, Texas Tech University, Lubbock, TX 79409-1061, USA

Received 2 September 2005; received in revised form 31 October 2005; accepted 13 December 2005
Available online 24 January 2006

Abstract

Classical trajectory simulations are performed for collisions between protonated diglycine (gly_2-H^+) and a diamond {1 1 1} surface at incident angles θ_i of 0° and 45°, with respect to the surface normal, and initial translational energies E_i of 35 and 70 eV. The trajectories are analyzed to determine how the orientation angle of the peptide ion and the surface impact site affect the collisional energy transfer. There are two distinct impact points on the surface on which the peptide ion can collide, hydrogen and carbon atoms, denoted as H- and C-sites. While the impact point plays little to no role in determining energy transfer, for $\theta_i = 0°$ the orientation angle of the peptide has a significant effect on energy transfer. When the peptide ion collides with its backbone vertical to the surface plane and, thus, with a C- or N-terminus approach, the internal energy change is a maximum and the final translational energy and surface internal energy change are at a minimum. When the peptide ion collides horizontally, the opposite occurs. In addition, for vertical collisions more energy is transferred to the peptide ion if the C-terminus first strikes the surface instead of the N-terminus. For non-perpendicular collisions, with $\theta_i = 45°$, the energy transfer efficiency is less sensitive to the peptide orientation. Peptide orientation becomes more important as E_i is increased.

Keywords: SID; Energy transfer; Projectile orientation

1. Introduction

Surface-induced dissociation (SID) is an important mass spectrometric technique for determining the primary structures of ions, and their energetics and dissociation mechanisms [1–5]. Both experimental [5,6] and chemical dynamics simulation [7–14] studies of SID have shown that the projectile ion receives a distribution of vibrational energy when it collides with the surface. An illustrative distribution is shown in Fig. 1 for collision of protonated diglycine (gly_2-H^+) with the diamond {1 1 1} surface [13]. Various attributes of the surface, projectile and collision may affect the dynamics of SID. Energy transfer to the projectile may be influenced by properties of both the surface and projectile, such as their structures, constituent atoms and functional groups. Also, though the collision has a fixed incident angle θ_i and energy E_i, the projectile has random orientations and random impact points on the surface, and each orientation and impact site may give rise to different SID dynamics. For many experiments, the beam of projectile ions overlaps many growth domains, with different azimuthal angles, and this may also affect the energy transfer.

For the research reported here classical trajectory simulations were used to study how projectile orientation and surface impact site affect energy transfer in collisions of gly_2-H^+ with diamond {1 1 1}; see Fig. 2. The peptide ion's orientation is determined by the angle between its backbone and the surface normal, which distinguishes whether the ion collides vertically or horizontally or with its C- or N-atom terminus first striking the surface. The center-of-mass of the peptide ion is directed to both H-atom and C-atom impact sites on the diamond {1 1 1} surface.

2. Computational methodology

The same computational procedure was used for the trajectories as in previous simulations of SID [7–14]. The classical

* Corresponding author. Tel.: +1 806 742 3152.
E-mail address: bill.hase@ttu.edu (W.L. Hase).
[1] Present address: Stephen F. Austin High School, Sugar Land, TX, USA.

1387-3806/$ – see front matter © 2005 Elsevier B.V. All rights reserved.
doi:10.1016/j.ijms.2005.12.020

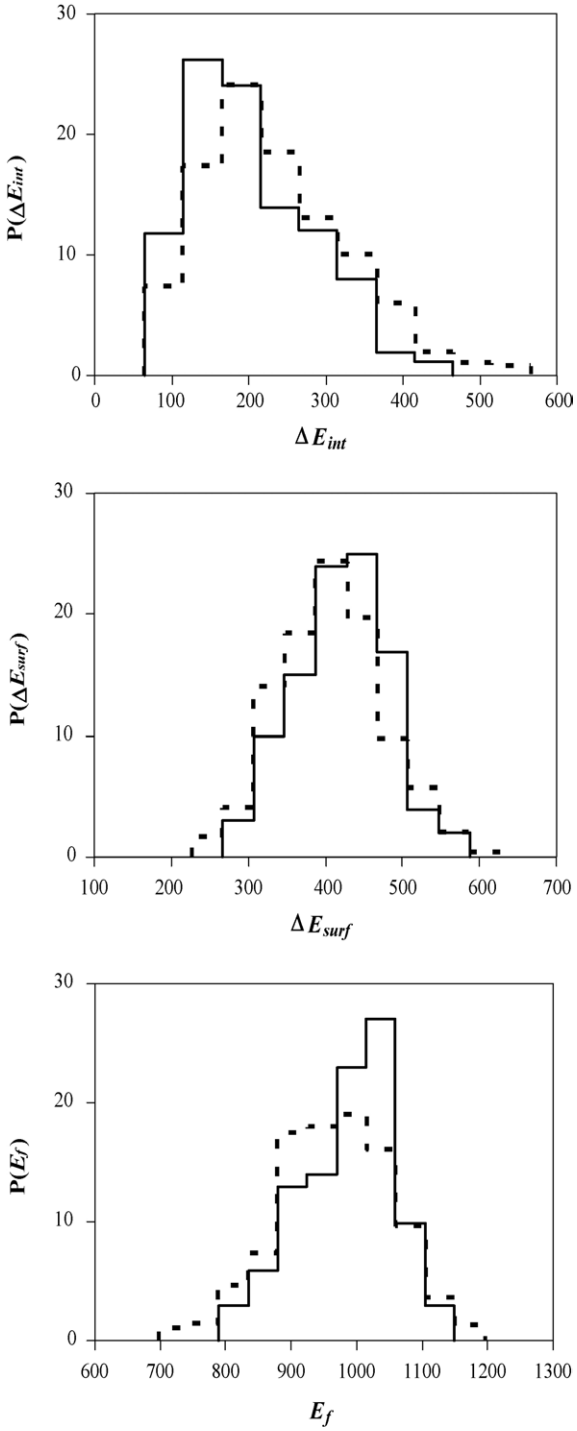

Fig. 1. Distributions of energy transfer to ΔE_{int}, ΔE_{surf}, and E_f for gly_2-H^+ collisions with diamond {1 1 1} surface at $E_i = 70$ eV (1614 kcal/mol) and $\theta_i = 45°$. Simulation with the Amber (- - -) and AM1 (—) models for the protonated diglycine intramolecular potential. Plots are taken from Ref. [13].

trajectory calculations were performed with the general chemical dynamics computer program VENUS [15]. The analytic function for the potential energy surface is expressed as

$$V = V_{\text{peptide}} + V_{\text{surface}} + V_{\text{peptide-surface}} \quad (1)$$

where V_{peptide} represents the peptide potential, V_{surface} the surface potential, and $V_{\text{peptide–surface}}$ the interaction potential

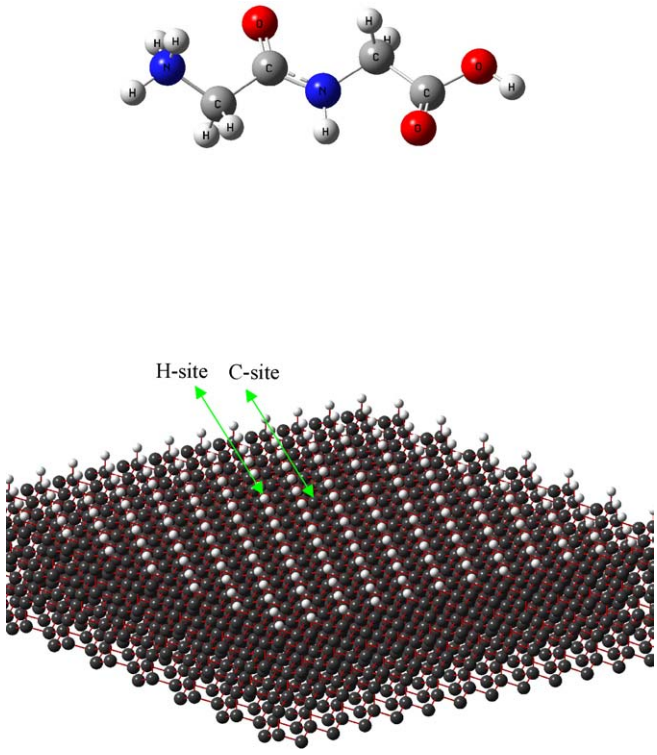

Fig. 2. Structures of the protonated diglycine ion and diamond {1 1 1} surface used for the simulations.

between the peptide and surface. The Amber94 [16] potential is used to describe V_{peptide}. V_{surface} is a quadratic potential, modified with Morse stretches, which fits the diamond phonon spectrum [17]. $V_{\text{peptide–surface}}$ is a sum of two-body potentials of the form

$$V_{XY} = A_{XY} \exp(-B_{XY} R_{ij}) + \frac{C_{XY}}{R_{ij}^6} \quad (2)$$

where X corresponds to the H-atoms or C-atoms of the surface and Y corresponds to the C, H, N, or O atoms of the peptide ion. The constants A, B, and C were determined by fitting high level ab initio results [10].

The diamond surface model is hydrogen terminated with eight layers of carbon atoms and a total of 1988 atoms. There are five heavy atoms added to the bottom of the surface so that the surface does not move upon collision with the peptide ion. The top view of the diamond {1 1 1} surface (Fig. 2) reveals two different atomic impact sites for collisions with the center-of-mass of the diglycine ion. One is a hydrogen atom on the outer-layer of the surface. The other is a carbon atom in the second surface layer and it is bonded to a carbon atom just below the surface hydrogen atom. The first impact site is denoted a H-site and second a C-site. In order to determine possible effects of the surface impact point on the efficiency of energy transfer to gly_2-H^+, one ensemble of classical trajectories was calculated with the center-of-mass of the diglycine ion directed towards the H-site and another with the ion directed towards the C-site. Ensembles of trajectories were also calculated with random impact sites for the colliding ion.

The peptide ion is randomly rotated in the trajectory initial conditions, which establishes the initial orientation of the ion with respect to the surface. To ensure the peptide ion approaches the surface in this orientation, the rotational temperature of the ion is set to 0 K. The initial orientation of the peptide ion is determined by defining a vector from the nitrogen atom of the protonated amino group to the hydroxyl oxygen atom of the carboxylic group. The angle between this vector and the vector normal to the diamond surface determines the orientation of the peptide ion.

The simulations were performed with both the surface and peptide ion's vibrational temperatures at 300 K. As discussed above, the ion's rotational temperature is 0 K. The ion's initial translational energy is 35 or 70 eV and its incident angle is 0° or 45° with respect to the surface normal. The trajectories were integrated with combined 4th order Runge–Kutta and 6th order Adams–Moulton algorithms. A step-size of 0.2 fs was used to integrate the classical equation of motion so that the total energy is conserved to within four significant figures. Five hundred trajectories were calculated for each of the collision sites.

3. Results and discussion

During the collision with the surface, part of the peptide ion's initial translational energy E_i is converted to surface vibrational energy E_{surf} and the peptide's internal vibrational/rotational degrees of freedom E_{int} according to

$$E_i = E_f + \Delta E_{surf} + \Delta E_{int} \quad (3)$$

where E_f is the final translational energy of the recoiling peptide ion. After each trajectory calculation, ΔE_{int}, ΔE_{surf} and E_f are determined. This information is then arranged in the form of histograms to determine the distribution of the internal energy change of the peptide ion $P(\Delta E_{int})$, the change in vibrational energy of the surface $P(\Delta E_{surf})$, and final translational energy $P(E_f)$ for simulations with both the H-atom and C-atom impact sites. The diglycine ion collides with no rotational energy and its initial orientation angle defines its orientation with respect to the surface as it collides. When the orientation angle is 0°, the protonated N-terminus of the peptide approaches the surface and collides vertically. When 180°, the C-terminus of the peptide ion approaches the surface and collides vertically. For an orientation angle of 90°, the peptide ion hits the surface horizontally.

3.1. Effect of impact site

The distributions for the internal energy changes of the peptide ion and the diamond surface, and for the final translational energy of the colliding projectile are shown in the Fig. 3 for collisions with both the H-atom and C-atom sites. Comparisons of the energy transfer distributions show no apparent differences for collisions with the two sites; i.e., features of the distributions for the two sites are very similar. The average percent energy transfers for collisions with the two sites are listed in Table 1 and seen to be identical within statistical uncertainties. These average energy transfers are the same as those reported previously [13] for collisions with random sites on the surface. (The previous simulation with random impact sites was repeated and the same results within statistical uncertainties were obtained.) The energy transfer distributions are insensitive to the impact point for protonated diglycine-diamond collisions. Apparently, the peptide ion is sufficiently large so, that when it collides with H-atom and C-atom sites on the diamond {1 1 1} surface, similar energy transfer distribution results.

Table 1
Average percent energy transfers for protonated diglycine collisions with the H-atom and C-atom sites on the diamond {1 1 1} surface

	Energy transfer		
	ΔE_{int}	ΔE_{suf}	E_f
E_i = 70 eV, θ_i = 0°			
H-site[a]	21.7 (±0.4)	41.0 (±0.3)	37.3 (±0.2)
C-site[a]	21.7 (±0.4)	40.8 (±0.3)	37.5 (±0.2)
Site ave.[b]	20	40	40
E_i = 70 eV, θ_i = 45°			
Site ave.[a]	15.1 (±0.3)	24.9 (±0.2)	60.0 (±0.2)
Site ave.[c]	15 (13)	25 (26)	60 (61)
E_i = 35 eV, θ_i = 0°			
Site ave.[a]	26.7 (±0.6)	29.1 (±0.3)	44.2 (±0.3)

The Amber94 potential is used for the peptide, unless noted otherwise. The surface is diamond {1 1 1}.

[a] Results presented here. The uncertainties are the standard deviation of the mean.

[b] Results from Ref. [13]. Random impact site were chosen for the collisions with the diamond {1 1 1} surface. Uncertainties were not reported.

[c] Results from Ref. [13]. Random impact sites were chosen for the collisions with the diamond {1 1 1} surface. The first set of percent energy transfers were calculated using Amber94 for the peptide potential as is done here. For the number in the parentheses AM1 was used for this potential. Uncertainties were not reported.

3.2. Effect of peptide ion orientation

The peptide ion orientation angle (Ψ_i) is the angle between the peptide backbone and surface normal as described above. It is calculated after the initial conditions are chosen with the peptide randomly orientated and, since no rotational energy is added for the peptide's initial conditions, it is maintained as the peptide approaches the surface. In Fig. 4 the internal energy changes for the peptide ion and surface, and the final translational energy, are plotted versus the orientation angle for collisions with both the H-atom and C-atom impact sites. Second-order polynomial fits were used to establish trend lines for the data and the fitting parameters are listed in Table 2. The number of points for the different orientation angles are in accord with the sine distribution for random orientations and a most probable angle of 90° [18].

The results clearly indicate that ΔE_{int}, ΔE_{surf} and E_f are sensitive to the orientation angle for collisions with both the H- and C-sites. As the angle approaches 0° or 180° (vertical orientation), the amount of translational energy transferred to the internal energy of the projectile ion tends to increase as compared to horizontal collisions with an orientation angle of 90°. As the internal energy of the peptide ion increases or decreases,

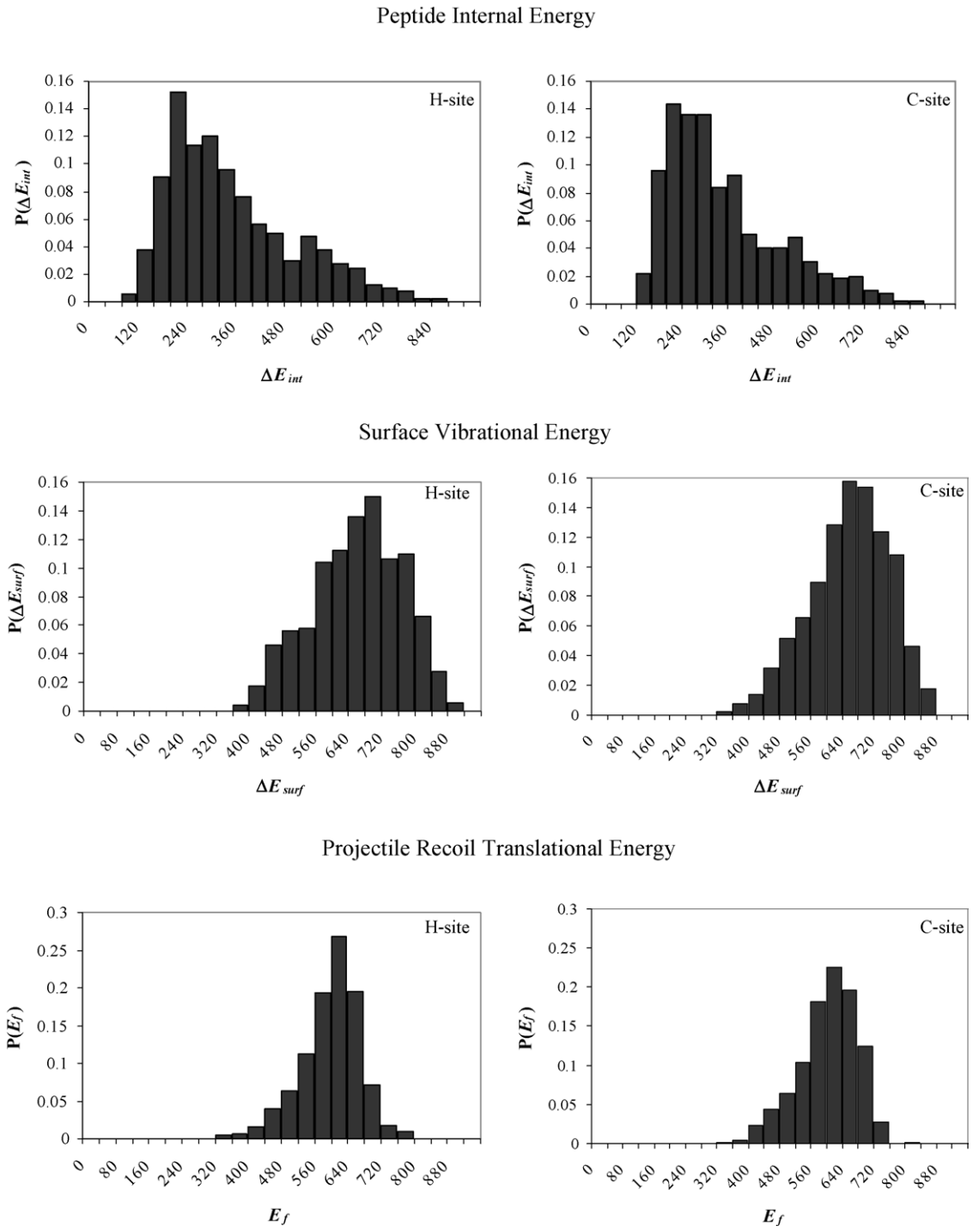

Fig. 3. Distributions of ΔE_{int}, ΔE_{surf}, and E_{f} for gly_2-H^+ collisions with the H-atom and C-atom sites of diamond {1 1 1}. Energy in the plots is in kcal/mol. $E_i = 70$ eV and $\theta_i = 0^\circ$.

the transfer of energy to the diamond surface or the peptide ion recoil energy decreases or increases, respectively. The average probabilities for these energy transfers are related by

$$\langle P(\Delta E_{\text{int}})\rangle + \langle P(\Delta E_{\text{surf}})\rangle + \langle P(E_{\text{f}})\rangle = 1 \quad (4)$$

Fig. 4 shows that, as $P(\Delta E_{\text{int}})$ increases (decreases), the decrease (increase) in $P(\Delta E_{\text{surf}})$ is more significant than that for $P(E_{\text{f}})$. However, there are differences in $P(E_{\text{f}})$ for the horizontal and vertical peptide ion collisions, which indicate that a complete theoretical understanding of the energy transfer will require a model that accurately describes the changes in the couplings between the probabilities $P(\Delta E_{\text{int}})$, $P(\Delta E_{\text{surf}})$ and $P(E_{\text{f}})$ as the peptide ion orientation changes.

An additional interesting feature of the energy transfer is that vibrational excitation of the peptide is more efficient if the C-

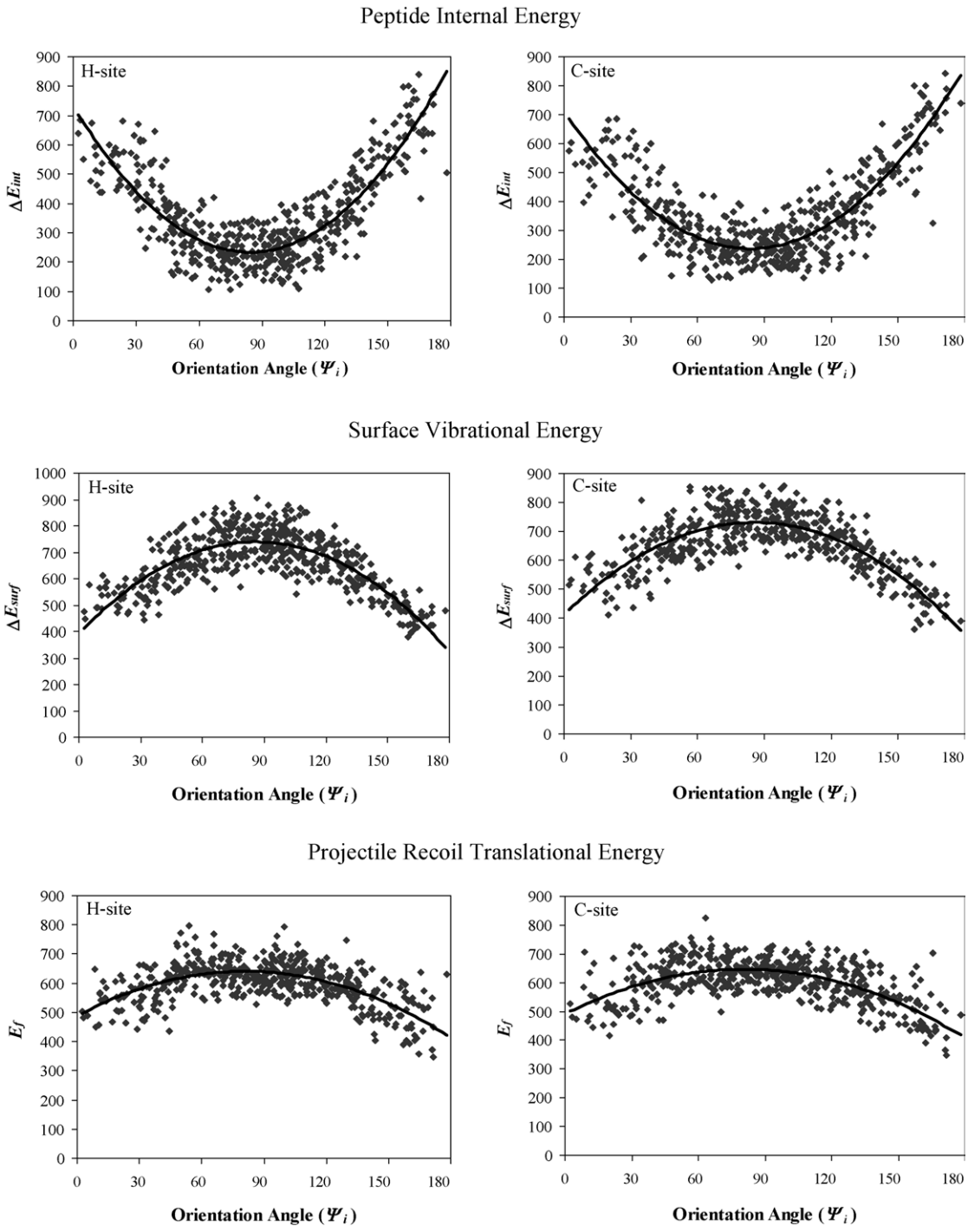

Fig. 4. Scatter plots, of the energy transfers in Fig. 3, vs. the gly_2-H^+ orientation angle. The curves are parabolic fits with the parameters listed in Table 2. Energy in the plots is in kcal/mol.

terminus of the peptide first strikes the surface, instead of the N-terminus. That this effect is seen for collisions with both the H-atom and C-atom surface sites suggests that it does not arise from features of the peptide-surface intermolecular potential, since it is expected to be different for the two surface sites. A likely origin of the different energy transfer efficiencies are difference in the peptide ion's intramolecular degrees of freedom excited by collisions between the surface and the two peptide termini.

3.3. Effect of peptide ion incident angle and collision energy

The above results for collisions of gly_2-H^+ with the diamond {1 1 1} surface are for $\theta_i = 0°$ and $E_i = 70$ eV and may be compared with the results of a previous study [13] which is identical except $\theta_i = 45°$. For this earlier work, random impact sites were chosen on the diamond {1 1 1} surface and the energy transfer distributions are plotted in Fig. 1. A comparison of the distribu-

Table 2
Parameters for parabolic fits of energy transfer vs. gly_2-H^+ orientation angle

Simulation[a]	ΔE_{intf}			ΔE_{sur}			E_f		
	Ψ_o	a	b	Ψ_o	a	b	Ψ_o	a	b
$E_i = 70$, $\theta_i = 0$, H-site	84.3	0.070	233.8	85.9	−0.047	739.3	80.9	−0.023	640.9
$E_i = 70$, $\theta_i = 0$, C-site	83.8	0.068	237.0	85.5	−0.044	730.5	80.4	−0.024	646.6
$E_i = 70$, $\theta_i = 45$, Site ave.	81.9	0.016	194.1	53.5	−0.005	424.2	94.9	−0.011	1001.8
$E_i = 35$, $\theta_I = 0$, Site ave.	85.10	0.046	139.8	87.3	−0.025	274.7	82.1	−0.021	391.9

The fit for ΔE_{int} is given by $\Delta E_{int} = a(\Psi_i - \Psi_o)^2 + b$. Analogous fits are made for ΔE_{surf} and E_f. Ψ_o has units of degrees, a units of degrees^{-2}, and b units of kcal/mol.
[a] E_i is in eV and θ_i in degrees.

tions in Fig. 1 for $\theta_i = 45°$, with those in Fig. 3 for $\theta_i = 0°$, shows that the distribution for a particular energy transfer are very similar in shape, but have different energy transfer efficiencies. The average energy transfers listed in Table 1 show that decreasing θ_i to 0° from 45° increases ΔE_{int} and ΔE_{surf} by 1.3 and 1.6, respectively, but decreases E_f by 1.5.

The previous simulation [13] for $\theta_i = 45°$ and collisions with random sites on the diamond {1 1 1} surface was repeated, with the peptide orientation recorded, to determine if peptide orientation has the same effect on the energy transfer efficiencies as found for $\theta_i = 0°$. The results are plotted in Fig. 5, where it is seen that vertical orientations tend to give more efficient excitation of the peptide than horizontal, with the most effective orientation being the C-terminus first striking the surface. These results are similar to those for an incident angle of 0°, but the overall effect of the peptide orientation is not as striking. The parameters for the parabolic fits to the points in Fig. 5 are given in Table 2. The a parameters for ΔE_{int} and ΔE_{surf} are significantly smaller for $\theta_i = 45°$ as compared to $\theta_i = 0°$.

As discussed above, changing the collision angle θ_i from 0 to 45° lowers the energy transfer efficiencies, and has an effect on the relationship between energy transfer and peptide orientation. Changing the collision angle varies the normal component of the collision energy according to $E_i^n = E_i \cos^2 \theta_i$ and, though energy transfer in protonated peptide + diamond {1 1 1} collisions does not scale according to E_i^n [13], the size of E_i^n is expected to have some effect on the energy transfer dynamics. Since collisions with $E_i = 70$ eV, $\theta_i = 45°$ and $E_i = 35$ eV, $\theta_i = 0°$ have the same value of E_i^n, it is of interest to investigate how protonated peptide orientation influences energy transfer for these two sets of initial conditions.

The effect of peptide orientation on the efficiencies of energy transfer for gly_2-H^+ collisions with diamond {1 1 1} for $E_i = 35$ eV and $\theta_i = 0°$ is shown in Fig. 6. Previous simulations [13] have shown that lowering E_i from 70 to 35 eV and maintaining θ_i at 0°, has a small effect on the percent transfer to ΔE_{int}, but decreases and increases, respectively, the percent transfers to ΔE_{surf} and E_f. As shown in Table 1, this result is also obtained here. Comparing the plots in Figs. 5 and 6 shows that peptide orientation has a more pronounced effect on the energy transfer efficiencies for the simulation at $E_i = 35$ eV, $\theta_i = 0°$ than the one at $E_i = 70$ eV, $\theta_i = 45°$. Since both simulations have the same normal component of E_i, apparently, enhanced surface roughness and anisotropy in the projectile-surface potential for the non-perpendicular collisions decreases the sensitivity of the energy transfer to the peptide orientation. Figs. 4 and 6 compare the effect of peptide orientation on the energy transfer for perpendicular collisions with different collision energies of 70 and 35 eV. The plots in the figures, and the a parameters in Table 2 for the parabolic fits, show that peptide orientation is more important at the higher E_i.

4. Summary

The work presented here and that published previously [1–14] illustrate there are important fundamental dynamical properties associated with the efficiencies of energy transfer when polyatomic projectile ions collide with hydrocarbon surfaces. The current study shows that the energy transfer efficiencies, for collisions of gly_2-H^+ with the diamond {1 1 1} surface, do not depend on where the peptide lands on the surface, but do depend on the orientation of the peptide's backbone with respect to the surface normal. Collisions with the backbone vertical enhance energy transfer to the peptide's vibration degrees of freedom. The most efficient energy transfer occurs when the peptide collides vertically and with the carboxylic group first striking the surface.

It is of interest to consider these results with what is known from previous computational and experimental studies regarding energy transfer in collisions of projectile ions with hydrocarbon surfaces. This information and that given here provides a basis for developing a theoretical model to describe the dynamics of SID. The previous studies show that the surface has an important effect on the energy transfer. Fluorinated alkyl thiolate self-assembled monolayer (F-SAM) and diamond surfaces transfer approximately a factor of two more energy to the projectile's internal degrees of freedom than do hydrogenated alkyl thiolate (H-SAM) surfaces [1,6,9,10,12]. The stiffness of the diamond surface may account for its efficiency to excite the projectile [9]. The high SID efficiency for F-SAM surfaces has been attributed to their projectile/target mass ratio, projectile/surface intermolecular potential, and/or rigidity of the fluorinated surface [19,20]. Studies of F-SAMs, with different extents of fluorination, indicate that it is the terminal –CF_3 group which is the major factor influencing energy transfer [21]. In collisions of benzene molecular ions with mixed SAMs consisting of both –OH and –CH_3 terminal groups, percent transfers to the projectile internal energy increases as the percent –OH termini increases [22]. The origin of this effect is unclear. It is not attributed to an increase in the surface stiffness due to hydrogen

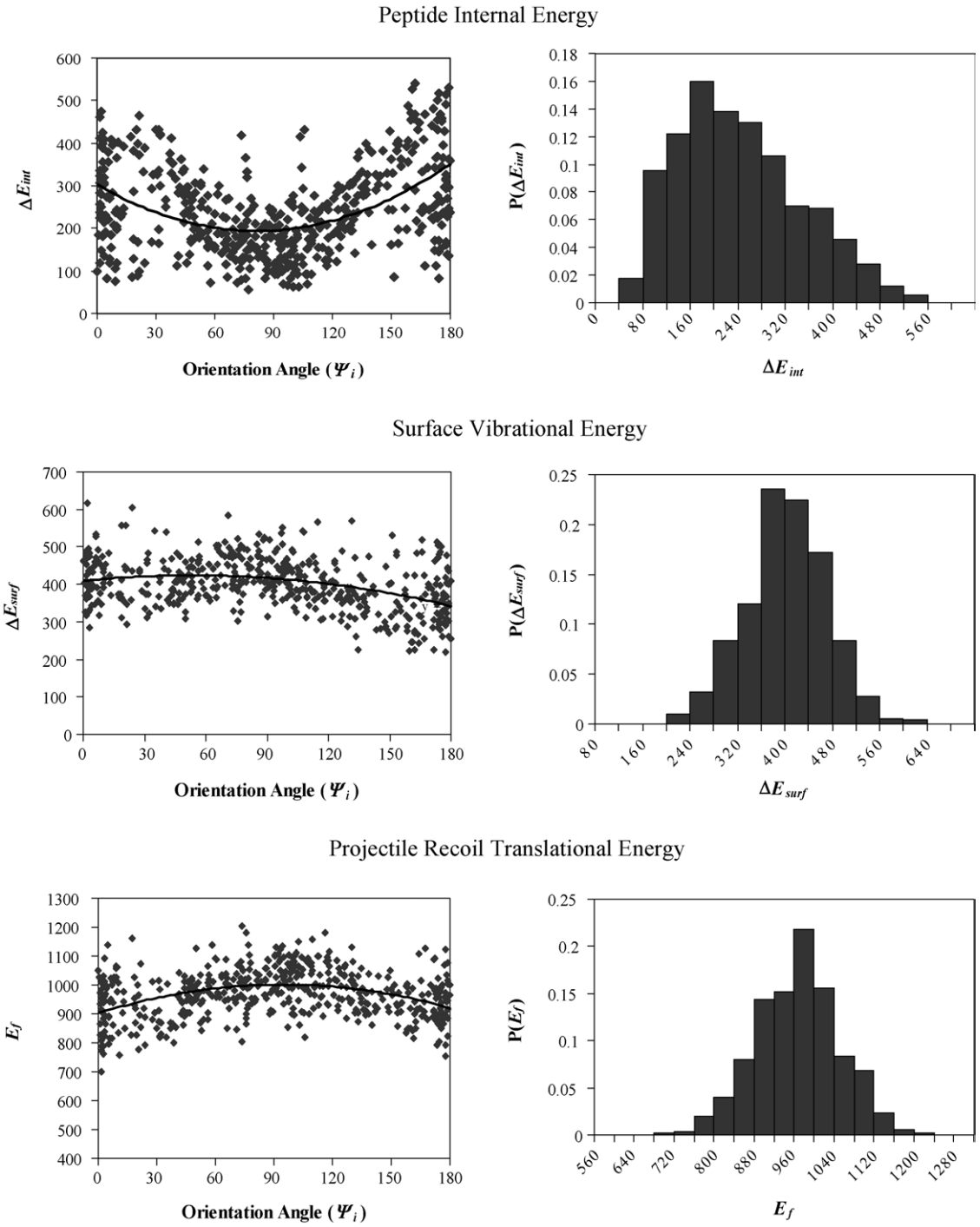

Fig. 5. Simulation results for $E_i = 70$ eV and $\theta_i = 45°$. Both energy transfer distributions and scatter plots of the energy transfer vs. gly_2-H^+ orientation angle are given. Energy in the plots is in kcal/mol.

bonding between the –OH groups, since the –OH and $–CH_3$ terminal groups are thought to randomly distribute when forming the surface and to not aggregate. An increase in surface stiffness and diminished energy transfer to the surface, has been observed for collisions of Ar atoms with surfaces terminated with hydrogen bonding functional groups [23–25].

The $P(\Delta E_{int})$ energy transfer distribution is broader for collisions with diamond {1 1 1} as compared to the F-SAM and H-SAM surfaces. This has been seen in simulations [9,10,12] of $Cr^+(CO)_6$ and gly_3-H^+ collisions with the H-SAM and diamond surfaces, and in experiments [6] of des-Arg^1-bradykinin colliding with the diamond, F-SAM, and H-SAM surfaces. The effect found here, that the energy transfer efficiency for gly_2-H^+ collisions with diamond {1 1 1} depends on the orientation of gly_2-H^+ as it impacts the surface, is expected to be a contributing factor to the width of $P(\Delta E_{int})$ for protonated peptide ion collisions with diamond surfaces. However, considerable additional work needs to be done to obtain a complete understanding of the

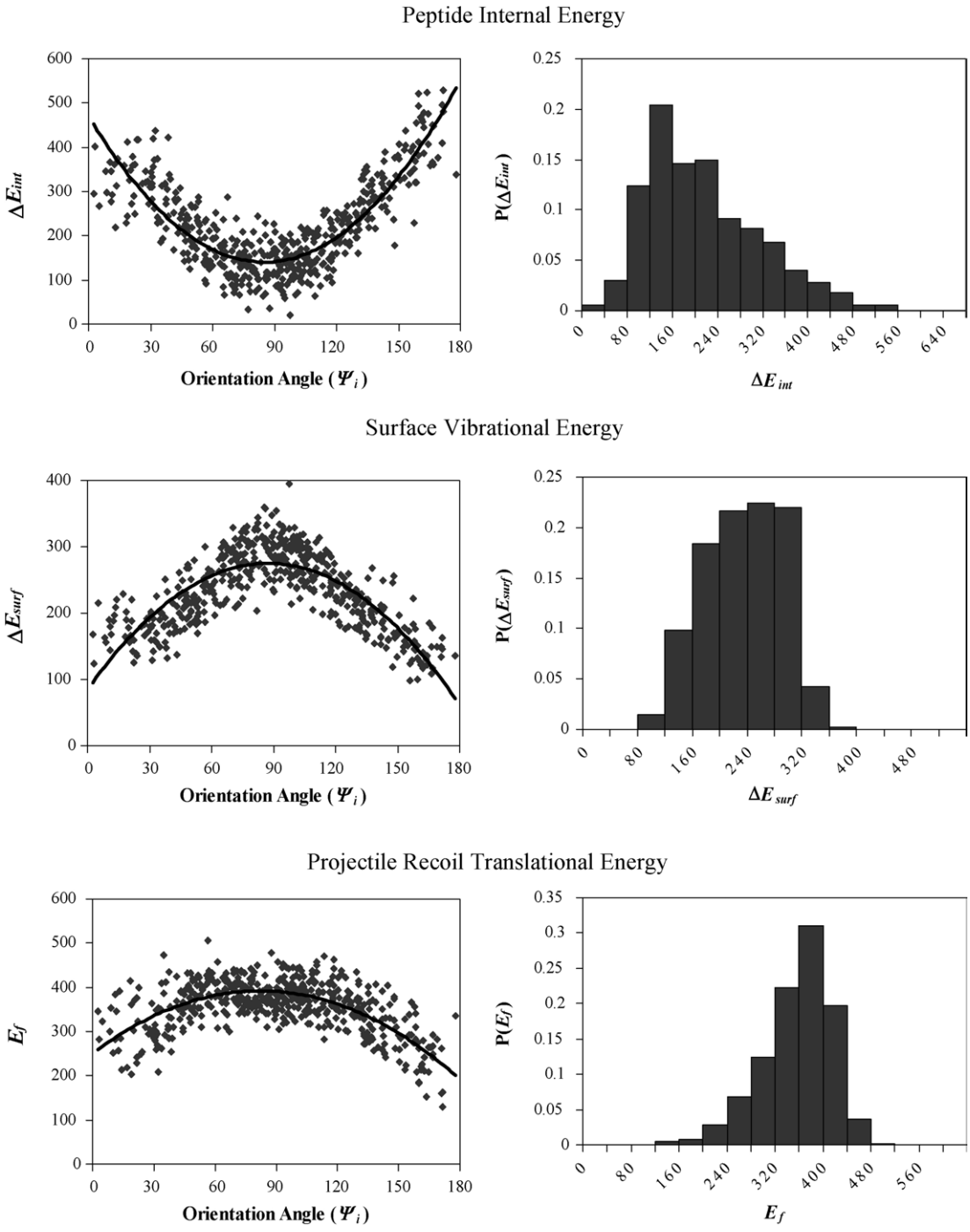

Fig. 6. Same as Fig. 5, except $E_i = 35$ eV and $\theta_i = 0^\circ$.

width and structure of $P(\Delta E_{\text{int}})$ for projectile ion collisions with hydrogenated surfaces. For $Cr^+(CO)_6$ collisions with diamond {1 1 1}, $P(\Delta E_{\text{int}})$ appears to become bimodal at large E_i [9,12] and this is not an obvious orientation effect, since $Cr^+(CO)_6$ has a symmetric octahedral structure.

The percent energy transfer to a protonated peptide ion projectile is remarkably insensitive to its size. Collisions of protonated dialanine (ala_2-H^+) and the protonated octapeptide des-Arg^1-bradykinin with the F-SAM give identical $E_i \rightarrow \Delta E_{\text{int}}$ energy transfer efficiencies [5,6]. Nearly identical percent energy transfers to E_{int} and E_{surf} are found for gly_3-H^+ and gly_5-H^+ colliding with either the H-SAM or diamond {1 1 1} surface [10]. For collisions with diamond with $E_i = 35$ eV and $\theta_i = 0^\circ$, the $E_i \rightarrow E_{\text{int}}$ energy transfer found from the simulations reported here is 27% for gly_2-H^+ and previous experiments reported 19% for des-Arg^1-bradykinin. A factor, which must be considered in exploring the relative insensitivity of the $E_i \rightarrow \Delta E_{\text{int}}$ percent transfer on peptide size, is that the peptide dihedral degrees of freedom may receive most of the internal energy. From simulations of gly_3-H^+ collisions with diamond {1 1 1}, it was found

that ~80% of the $E_i \rightarrow \Delta E_{int}$ transfer goes to the dihedrals [10]. The energy potentially available in SID, to dissociate a projectile, may be increased by increasing the temperature of the surface and/or the projectile, as well as increasing the collision energy E_i. Experiments have shown that the $E_i \rightarrow \Delta E_{int}$ percent energy transfer is unaffected by raising the projectile temperature [26]. Simulations [27] give the same result, and also show the energy transfer is unaffected by the surface temperature.

Another important feature of SID energy transfer dynamics is the overall insensitivity of the $E_i \rightarrow \Delta E_{int}$ percent energy transfer to changes in E_i. Experiments of both ala_2-H^+ and des-Arg^1-bradykinin SID indicate that this percent energy transfer does not change for E_i in the ranges of 5–23 and 10–100 eV [5,6]. Simulations give a similar result, where for gly_2-H^+ + diamond {1 1 1} collisions at $\theta_i = 45^\circ$, the percent energy transfer to ΔE_{int} only changes from 16 to 13% as E_i is increased from 5 to 110 eV [13]. Such a small change may not be detectable in the RRKM models used to interpret the experiments [5,6].

The orientation effect found in these simulations, for the efficiency of energy transfer in SID, suggests the conformation of the peptide may also influence the energy transfer efficiency. Such a conformational effect was observed in trajectory simulations of CID [28], but not in a more limited trajectory study of SID [10]. For the latter, it was found that extended and folded conformations of gly_3-H^+ have similar energy transfer efficiencies when they collide with diamond {1 1 1} and H-SAM surfaces. A more extensive simulation study, consisting of a broad range of conformations and peptide size, seems appropriate in light of the work reported here. Investigating in more detail a possible conformation effect on energy transfer in SID is important, since some manipulation of the conformation of ions is possible in electrospray ionization (ESI) [29].

In conclusion, previous experiments and simulations have illustrated there is a wealth of detail in the energy transfer dynamics of SID. The results reported here have added another complexity, which may be helpful in developing a theoretical model for the dynamics of SID.

Acknowledgements

This material is based upon work supported by the National Science Foundation under Grant No. 0412677 and the Robert A. Welch Foundation under Grant No. D-0005. The authors wish to thank Jean Futrell, Julia Laskin, and Vicki Wysocki for valuable discussions concerning the dynamics of SID. Jing Brian Zhou was a 2005 Robert A. Welch Summer Research Scholar.

References

[1] M.R. Morris, D.E. Riederer Jr., B.E. Winger, R.G. Cooks, T. Ast, C.E.D. Chidsey, Int. J. Mass Spectrom. Ion Processes 122 (1992) 181.
[2] A.L. McCormack, A. Somogyi, A.R. Dongré, V.H. Wysocki, Anal. Chem. 65 (1993) 2859.
[3] J.A. Burroughs, S.B. Wainhaus, L. Hanley, J. Phys. Chem. 98 (1994) 10913.
[4] J. Kubišta, Z. Dolejšek, Z. Herman, Eur. Mass Spectrom. 4 (1998) 311.
[5] J. Laskin, E. Denisov, J.H. Futrell, J. Am. Chem. Soc. 122 (2000) 9703.
[6] J. Laskin, J.H. Futrell, J. Chem. Phys. 119 (2003) 3413.
[7] D.G. Schultz, S.B. Wainhaus, L. Hanley, P. de Sainte Claire, W.L. Hase, J. Chem. Phys. 106 (1997) 10337.
[8] S.B.M. Bosio, W.L. Hase, Int. J. Mass Spectrom. Ion Processes 174 (1998) 1.
[9] O. Meroueh, W.L. Hase, Phys. Chem. Chem. Phys. 3 (2001) 2306.
[10] O. Meroueh, W.L. Hase, J. Am. Chem. Soc. 124 (2002) 1524.
[11] S.O. Meroueh, Y. Wang, W.L. Hase, J. Phys. Chem. A 106 (2002) 9983.
[12] K. Song, O. Meroueh, W.L. Hase, J. Chem. Phys. 118 (2003) 2893.
[13] J. Wang, S.O. Meroueh, Y. Wang, W.L. Hase, Int. J. Mass Spectrom. 230 (2003) 57.
[14] Y. Wang, W.L. Hase, K. Song, J. Am. Soc. Mass Spectrom. 14 (2003) 1402.
[15] W.L. Hase, R.J. Duchovic, X. Hu, A. Komornicki, K.F. Lim, D.-H. Lu, G.H. Peslherbe, K.N. Swamy, S.R. Vande Linde, L. Zhu, A. Varandas, H. Wang, R. Wolf, J. QCPE 16 (1996) 671.
[16] W.D. Cornell, P. Cieplak, C.I. Bayly, I.R. Gould, K.M. Merz, D.M. Ferguson, D.C. Spellmeyer, T. Fox, J.W. Caldwell, P.A. Kollman, J. Am. Chem. Soc. 117 (1995) 5179.
[17] K.C. Hass, M.A. Tamor, T.R. Anthony, W.F. Banholzer, Phys. Rev. B 45 (1992) 7171.
[18] G.H. Peslherbe, H. Wang, W.L. Hase, A chapter in Monte Carlo methods in chemical physics, in: D.M. Ferguson, J.I. Siepman, D.G. Truhlar (Eds.), Advances in Chemical Physics, vol. 105, Wiley, New York, 1999, p. 171.
[19] S.R. Cohen, R. Naaman, J. Sagiv, Phys. Rev. Lett. 58 (1987) 1208.
[20] J. Wang, W.L. Hase, J. Phys. Chem. B 109 (2005) 8320.
[21] D.L. Smith, V.H. Wysocki, R. Colorado Jr., O.E. Shmakova, M. Graupe, T.R. Lee, Langmuir 18 (2002) 3895.
[22] D.L. Smith, R. Selvan, V.H. Wysocki, Langmuir 19 (2003) 7302.
[23] S.F. Shuler, G.M. Davis, J.R. Morris, J. Chem. Phys. 116 (2002) 9147.
[24] B.S. Day, S.F. Shuler, A. Ducre, J.R. Morris, J. Chem. Phys. 119 (2003) 8084.
[25] M.K. Ferguson, J.R. Lohr, B.S. Day, J.R. Morris, Phys. Rev. Lett. 92 (2004) 073201.
[26] A. Qayyum, Z. Herman, T. Tepnual, C. Mair, S. Matt-Leubner, P. Scheier, T.D. Märk, J. Phys. Chem. A 108 (2004) 1.
[27] A. Rahaman, O. Collins, C. Scottt, J. Wang, W.L. Hase, in preparation.
[28] O. Meroueh, W.L. Hase, J. Phys. Chem. A 103 (1999) 3981.
[29] J.B. Fenn, M. Mann, C.K. Meng, S.F. Wong, C.M. Whitehouse, Science 246 (1989) 64.